The role of declining Arctic sea ice in recent decreasing terrestrial Arctic snow depths

Hotaek Park [a,*], John E. Walsh [b], Yongwon Kim [b], Taro Nakai [b], Tetsuo Ohata [a]

[a] Research Institute for Global Change, JAMSTEC, 2-15 Natsushimacho, Yokosuka 237-0061, Japan
[b] International Arctic Research Center, University of Alaska Fairbanks, Fairbanks, AK 99775, USA

Abstract

The dramatic decline in Arctic sea ice cover is anticipated to influence atmospheric temperatures and circulation patterns. These changes will affect the terrestrial climate beyond the boundary of the Arctic, consequently modulating terrestrial snow cover. Therefore, an improved understanding of the relationship between Arctic sea ice and snow depth over the terrestrial Arctic is warranted. We examined responses of snow depth to the declining Arctic sea ice extent in September, during the period of 1979–2006. The major reason for a focus on snow depth, rather than snow cover, is because its variability has a climatic memory that impacts hydrothermal processes during the following summer season. Analyses of combined data sets of satellite measurements of sea ice extent and snow depth, simulated by a land surface model (CHANGE), suggested that an anomalously larger snow depth over northeastern Siberia during autumn and winter was significantly correlated to the declining September Arctic sea ice extent, which has resulted in cooling temperatures, along with an increase in precipitation. Meanwhile, the reduction of Arctic sea ice has amplified warming temperatures in North America, which has readily offset the input of precipitation to snow cover, consequently further decreasing snow depth. However, a part of the Canadian Arctic recorded an increase in snow depth driven locally by the diminishing September Arctic sea ice extent. Decreasing snow depth at the hemispheric scale, outside the northernmost regions (i.e., northeastern Siberia and Canadian Arctic), indicated that Arctic amplification related to the diminishing Arctic sea ice has already impacted the terrestrial Arctic snow depth. The strong reduction in Arctic sea ice anticipated in the future also suggests a potential long-range impact on Arctic snow cover. Moreover, the snow depth during the early snow season tends to contribute to the warming of soil temperatures in the following summer, at least in the northernmost regions.
© 2012 Elsevier B.V. and NIPR. All rights reserved.

Keywords: Sea ice extent; Snow depth; Land surface model; Arctic amplification; Climatic memory

1. Introduction

The Arctic is warming faster than other regions of the Earth. The extent of the warming is exceeding values predicted by climate models (IPCC, 2008). A number of significant changes related to the warming have been found in climatic, ecological, and hydrological systems over the Arctic terrestrial region during the past few decades (Sturm et al., 2001; Serreze et al., 2000; Peterson et al., 2002). Most climate models also project that warming will continue, and thus the risks associated with these changes will further increase in the future.

* Corresponding author. Tel.: +81 46 867 9292.
  E-mail address: park@jamstec.go.jp (H. Park).

Using *in situ* observations for 1875–2008, Bekryaev et al. (2010) found that air temperatures over the northern polar area have recorded the largest increase during the winter season. The warming winter temperature could affect the processes of snow accumulation and ablation over the Arctic. Recent studies have indicated a significant decrease in the snow-covered area over the Arctic during winter, in response to the increasing air temperature (Brown, 2000; McCabe and Wolock, 2010). The decrease in snow depth (SND) during the past few decades had also been identified by observation (Dyer and Mote, 2006) and simulation (Park et al., 2012a). In contrast, long-term *in situ* observations in northern Eurasia identified increasing SND trends (Bulygina et al., 2009; Kitaev et al., 2005). However, earlier occurrence of Arctic snowmelt and a substantial retreat of snow cover have been found during spring, based on satellite image analyses (Brown et al., 2010; Shi et al., 2011). The retreat of snow cover during spring is likely to contribute to increases in air temperature through positive radiative feedbacks (Groisman et al., 1994).

Snow impacts regional radiative and energy budgets, atmospheric circulation, and soil hydrothermal conditions (Groisman et al., 1994). Changes in SND therefore have climatic and hydrologic implications. Moreover, SND is a useful indicator of climate changes. The decrease in winter SND may not be influenced by just the increased winter temperature. The winter SND depends largely on the conditions during the early snow season when snow starts to accumulate. Arctic warming has also resulted in later snow accumulation in autumn (Park et al., 2012a; Ye, 2001). Screen and Simmonds (2010) found that the warming in autumn is closely related to the retreat of Arctic sea ice. Of particular interest is the 40% reduction of sea ice extent (SIE) in summer 2007 compared to the local climatology (Comiso et al., 2008). This retreat is faster than the sea ice loss projected by climate models (IPCC, 2008), and it is assumed that the influence of the reduced autumn sea ice could accelerate winter Arctic warming. In reality, the decrease in the area of autumn Arctic sea ice is linked to changes in the Northern Hemisphere atmospheric circulation during winter (Cohen et al., 2012; Liu et al., 2012). Francis et al. (2009) documented that the atmosphere 'remembers' a reduction in summer sea ice cover, causing warming and destabilization of the lower troposphere in the following autumn and winter. These atmospheric changes will in turn affect the terrestrial climate and hydrology as a result of the atmosphere land coupling. Ghatak et al. (2010) found that the increasing snow cover over Siberia during autumn and early winter was correlated with the decreasing September Arctic sea ice over the Pacific sector.

Snow cover influences energy and radiation budgets over the land surface through albedo feedback during periods when snow is present. SND has an important hydrological effect of enhancing soil moisture, which persists into the following summer, contributing to evaporation and river discharge. Furthermore, the history of snow evolution greatly influences the soil temperature in the following year through the insulation effect. That is, SND-hydrothermal effects appear after snowmelt. Considering the atmosphere ocean land coupling in the Arctic system, the effect of sea ice on SND is likely to persist through to the following summer. Therefore, it is necessary to investigate the relationship between SND in the early snow season and the preceding summer's sea ice. Understanding this relationship may be important to projecting soil temperature and moisture in the following summer. Climate models have projected a rapid decline of sea ice in the future (IPCC, 2008). The projections suggest future changes in Arctic snow and therefore in hydrological processes in the following summer.

The main objective of this study was to explore how the decline in Arctic September sea ice extent (SIE) is linked to anomalously large SND variations over the Arctic terrestrial region during 1979–2006. We focused on SND during the autumn and winter seasons, which represent the snow accumulation period, and on September sea ice, which is the month with a climatological minimum of sea ice cover. Therefore, observed variations in SND could include any signals of changes emerging in the link between snowpack and decreasing SIE. The reason why we focused on SND, rather than snow cover, is because the influence of SND can persist through to the following summer as the aforementioned climate memory. Most of the previous studies that have examined the relationship between changing sea ice cover and snow have focused on snow cover, linked to changes in the Northern Hemisphere atmospheric climate in the winter (Francis et al., 2009; Liu et al., 2012; Cohen et al., 2012). Park et al. (2012a) described the spatiotemporal trends and variability in SND and snow cover extent over the Arctic terrestrial regions during 1948–2006, based on a simulation by the land surface model CHANGE (Park et al., 2011). Here we extend the previous study, combining it with observational data for SIE.

2. Model description

CHANGE is a state-of-the-art process-based model of the land surface. It calculates heat, water, and

radiation fluxes over soil, canopy, and snow surfaces in the atmosphere land system, as well as soil thermal and hydrologic states, including an explicit treatment of soil freeze/thaw phase changes, and carbon and nitrogen fluxes in ecosystems. Permafrost dynamics were improved by representing the effects of soil organic matter changes with time, depending on the simulated soil carbon budget according to soil thermal and hydrological properties. Soil depth was extended to 30.5 m to capture the thermal inertia provided by deep ground, considering a vertically heterogeneous soil texture distribution. Evapotranspiration was calculated as the sum of partitioned transpiration, interception, and soil evaporation. Transpiration was greatly dependent on variations in the leaf area index and root amounts, for which the spatiotemporal variations were also simulated by the model for every time step.

The CHANGE model represents snow dynamic processes using a two-layer energy and mass balance approach. The energy balance is used to simulate snowmelt, refreezing, and changes in the snowpack heat content. In calculating the radiation balance, the shortwave radiation is divided into direct beam and diffuse radiation because the canopy and soil have different spectral properties for individual spectral bands. The albedo for the canopy and soil is also calculated by a two-stream approximation method, in which the ground albedo for the two components is determined by weighting the soil and snow albedos. The mass balance components represent snow accumulation/ablation, changes in snow water equivalent, and water yield from the snowpack. The snowpack compacts with snowfall, which increases gravitational settling and also contributes to the densification of the snowpack. Therefore, compaction represents the sum of metamorphism and overburden, which also influences snow density. The estimated snow density along with the simulated snow water equivalent is used to estimate snow depth. A part of snowfall is primarily intercepted by the canopy when overstory is present. The processes of snow interception are calculated by the algorithm of Storck et al. (2002). The CHANGE model incorporates a vegetation dynamics model, which is useful to assess the effect of changing vegetation structure on the land surface processes. Park et al. (2011) provided a full description of the CHANGE model.

3. Datasets

We forced the CHANGE model with a gridded climate dataset of 0.5° latitude/longitude and daily resolutions over the global land area for the period 1948–2006. Because the dataset was extensively described by Hirabayashi et al. (2008) and Park et al. (2012a), only a brief description is provided here. The gridded products for air temperature and precipitation (P_G) were interpolated based on various monthly station observations. The temperature data were obtained from the Climatic Research Unit (CRU) Ts 2.1, the Global Historical Climatology Network (GHCN), and the NOAA Climate Prediction Center (CPC) Climate Anomaly Monitoring System (CAMS) datasets, and P_G data were obtained from NOAA CPC station data and the Global Precipitation Climatology Centre (GPCC) ver. 5. A stochastic weather generator was used to disaggregate monthly climatic variables into a daily time series. The daily shortwave radiation was derived from the surface radiation budget (SRB). The wind speed was obtained from the European Centre for Medium-Range Weather Forecasts (ECMWF) 40-year reanalysis (ERA-40); the wind speed at 2.5° resolution was interpolated to 0.5° grids within the 2.5° × 2.5° grid.

Initial conditions for the soil thermal and hydrological regimes and vegetation components were determined by a spin-up, running from an assumed state of no snow, no soil carbon, and a prescribed minimum of vegetation carbon. The soil moisture was initially set to the field capacity of the soil type for the top 5.5 m depth and to 90% of saturation for the remaining layers, and the vertical distribution of soil temperature was linearly interpolated using the air temperature at the simulation start date and annual mean temperature. The spin-up was run for approximately 420 years by looping repeatedly through a record of the initial 20 years of meteorological data. Total ecosystem carbon was used as a primary diagnostic for the spin-up run. The total ecosystem carbon was averaged over the 20-year period for each cycle. As the trend in the averaged total ecosystem carbon over time reached a threshold value (0.1 g C/m^2/yr), the spin-up was completed. Any influences of the initial conditions on the other processes were generally offset during the spin-up. The CHANGE model does not include glaciers yet, and thus Greenland was excluded from the simulation. The whole land region >45°N was set for the simulation.

The SIE data retrieved from the Scanning Multichannel Microwave Radiometer and the Special Sensor Microwave/Imager using the NASA team algorithm (Fetterer et al., 2002) were obtained from the National Snow and Ice Data Center (NSIDC). A SIE data set is available at a spatial resolution of 25 km; but we used

the mean SIE time series available from the NSIDC Sea Ice Index (http://nsidc.org/data/seaice_index/).

We also used the Climate Research Unit (CRU) air temperature and P_G data sets, version 3.0 (http://www.cru.uea.ac.uk/cru/data/hrg/), which consist of land-based monthly data on a regular 0.5° longitude/latitude global grid. The CRU data were used to investigate the influences of decreasing SIE on land surface temperature and P_G for the study period and the subsequent effect on SND.

4. Results

4.1. Sea ice extent and climate

A diminishing SIE for the period of the available satellite data record was conspicuous in all months, with the minimum extent typically occurring in September. Both the actual and detrended ice extents are shown in Fig. 1. The detrended values exclude effects of the interannual variability in ice extent alone. The SIE decreased about 21.3% ($p < 0.0001$ by Mann−Kendall test) during the period of 1979−2006. The rate of retreat for SIE outpaced the projections simulated by Intergovernmental Panel on Climate Change Fourth Assessment Report (IPCC AR4) climate models in response to greenhouse warming (Stroeve et al., 2011). An extreme decline in sea ice cover since 2005 was found in an extended region (the Beaufort Sea, Chukchi Sea, East Siberian Sea, Laptev Sea, and Kara Sea) compared with the ice edge for the minimum conditions averaged over 1979−2006. The SIE was at a minimum in 2007 and declined further in the East Siberian Sea compared with 2005; however, it recovered in the Sea around the Taymyr Peninsula (e.g., Comiso et al., 2008). When the amount of highly reflective sea ice is reduced, the input of solar heat into the ocean is increased, leading to increases in heat

storage in the upper ocean. As a result, the warm upper ocean retards the recovery of sea ice coverage in autumn and early winter. Furthermore, during this period the anomalously warm, ice-free ocean water enhances the heat and moisture fluxes between the surface and atmosphere, which are extended to the terrestrial Arctic with implications for atmospheric circulation (Screen and Simmonds, 2010).

The Arctic Oscillation (AO), which is a leading mode of wintertime climate variability in the Northern Hemisphere, has exhibited a decreasing trend since 1988 ($p < 0.032$) (Fig. 1). The AO is closely correlated to Eurasian snow cover in the autumn, with a higher autumn snow cover generally leading to a negative AO in the lower troposphere in winter (Cohen et al., 2007). The negative AO trend favors anomalously cold temperatures over the eastern United States and northern Eurasia in winter (Thompson and Wallace, 1998).

The wintertime (December−February) surface air temperature (SAT) during 1979−2006 exhibited a dipole pattern in its trend between Eurasia (EUR) and North America (NA) (Fig. 2a). Winter warming was significant over most of NA except for western Alaska, and the magnitude of the warming tended to be larger in the northern regions than in the south. The maximum increase in SAT over NA was found in eastern Alaska with a warming trend of 1.6 °C/decade. SAT in the Scandinavian Peninsula also exhibited a strong increasing trend. However, conspicuous negative trends were identified over far eastern and north-central Siberia. Interestingly, the trend of SAT in EUR also revealed large magnitude changes in the northern regions, as in NA. Precipitation exhibited regionally heterogeneous trends (Fig. 2b). In NA, significant trends of P_G were found at the western seashore regions and eastern Canada. In EUR, P_G trends showed clear differences between the eastern and western regions. Western EUR exhibited a strong decrease with locally positive trends, whereas eastern EUR generally retained the normal state of P_G, with the exception of the Far East.

4.2. Snow depth variability

The averaged snow depth during winter in both NA and EUR indicated a decreasing trend, which was statistically significant only in NA (Fig. 3). From 1954 to the early 1970s, both continents retained a value of SND considered to be above normal. Thereafter, SND in EUR decreased and then continued a pattern of normal anomalies until 2000, when it began to decrease again. In NA, SND exhibited an obvious
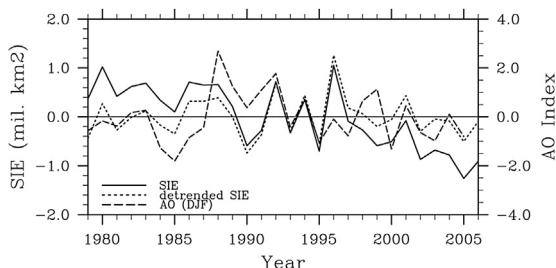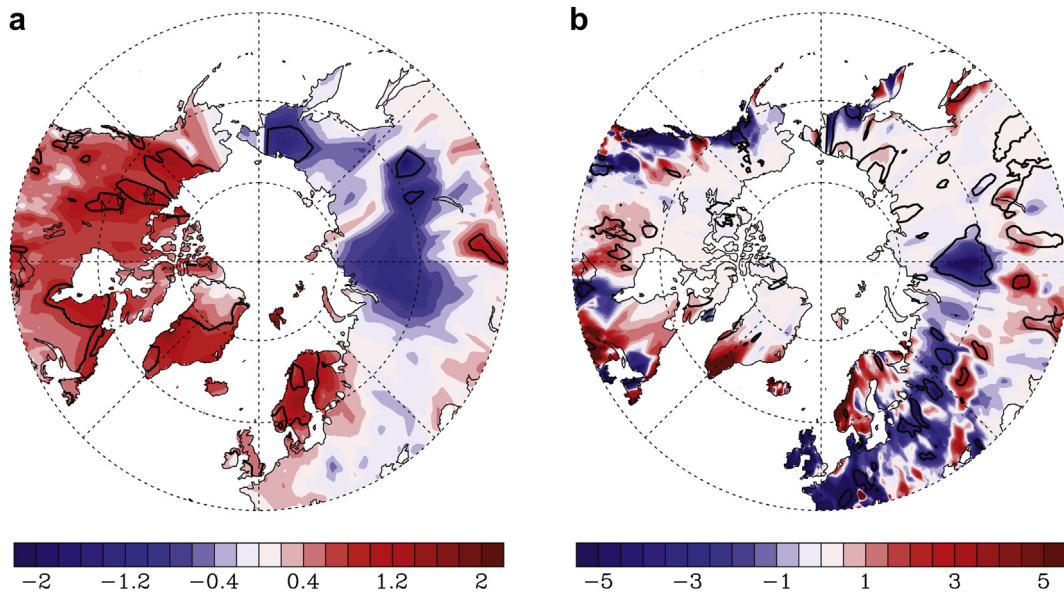

Fig. 1. Time series of the Arctic September sea ice extent, the detrended sea ice extent anomalies, and the Arctic Oscillation index in winter (December−February, DJF) during the period of 1979−2006.

Fig. 2. Trends of winter (December—February) air temperature (°C/decade) (a) and precipitation (mm/month/decade) (b) during the period of 1979—2006. Regions within contours denote points above the 95% confidence level.

decreasing trend ($p < 0.0001$) from 1971 onward. The decrease in the 1990s and 2000s was particularly strong, reaching a maximum of 10 cm in 1997. Dyer and Mote (2006) recorded a locally significant decrease (-0.25 cm yr^{-1}) in the SND of northwestern Canada, in response to rising air temperature, during the period of 1960—2000. The maximum SND in the western prairie provinces of Canada also decreased by 31—64% during the period of 1956—2003 (Schindler and Donahue, 2006). On the other hand, *in situ* observations in EUR have shown increasing trends of winter SND (Bulygina et al., 2009; Kitaev et al., 2005),
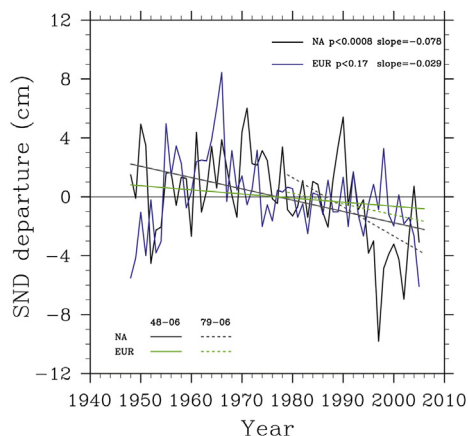

Fig. 3. Interannual variability of winter snow depth in Eurasia and North America during the period of 1948—2006.

which is contrary to our result. The period of 1979—2006, for which satellite SIE data are available, also exhibited statistically significant decreasing trends in SND for both NA ($p < 0.0004$, slope = -0.21) and EUR ($p < 0.02$, slope = -0.08) (Fig. 3).

Monthly SND data for EUR and NA show evident decreases during the past two decades (Fig. 4a, b). The decreases are stronger in NA than in EUR. In NA, the negative trend in most months during the period of 1979—2006 was at least twice as large as during the 1948—2006 period. The largest decreases were identified during the winter months (i.e., December—March), which was likely to be a combined effect of increased SAT (Fig. 4f) and less P_G (Fig. 4h). The increase in SAT in January—March during the 1979—2006 period was lower than that during the 1948—2006 period (Fig. 4f). In spite of such temperature conditions, SND decreased substantially, which seems to be related to the lower P_G (Fig. 4h). The negative trend of SND in April was the largest (i.e., 2.3 cm/decade), which was also influenced by a higher SAT (Fig. 4f) and less P_G (Fig. 4h). Satellite and *in situ* observations have revealed reductions in spring snow cover over NA during recent decades (Brown et al., 2010). On the other hand, the autumnal P_G in NA increased (Fig. 4h), while SND decreased, which was also associated with the warm SAT (Fig. 4f).

In EUR, SND also exhibited negative trends in most months during the two periods, with the exception of
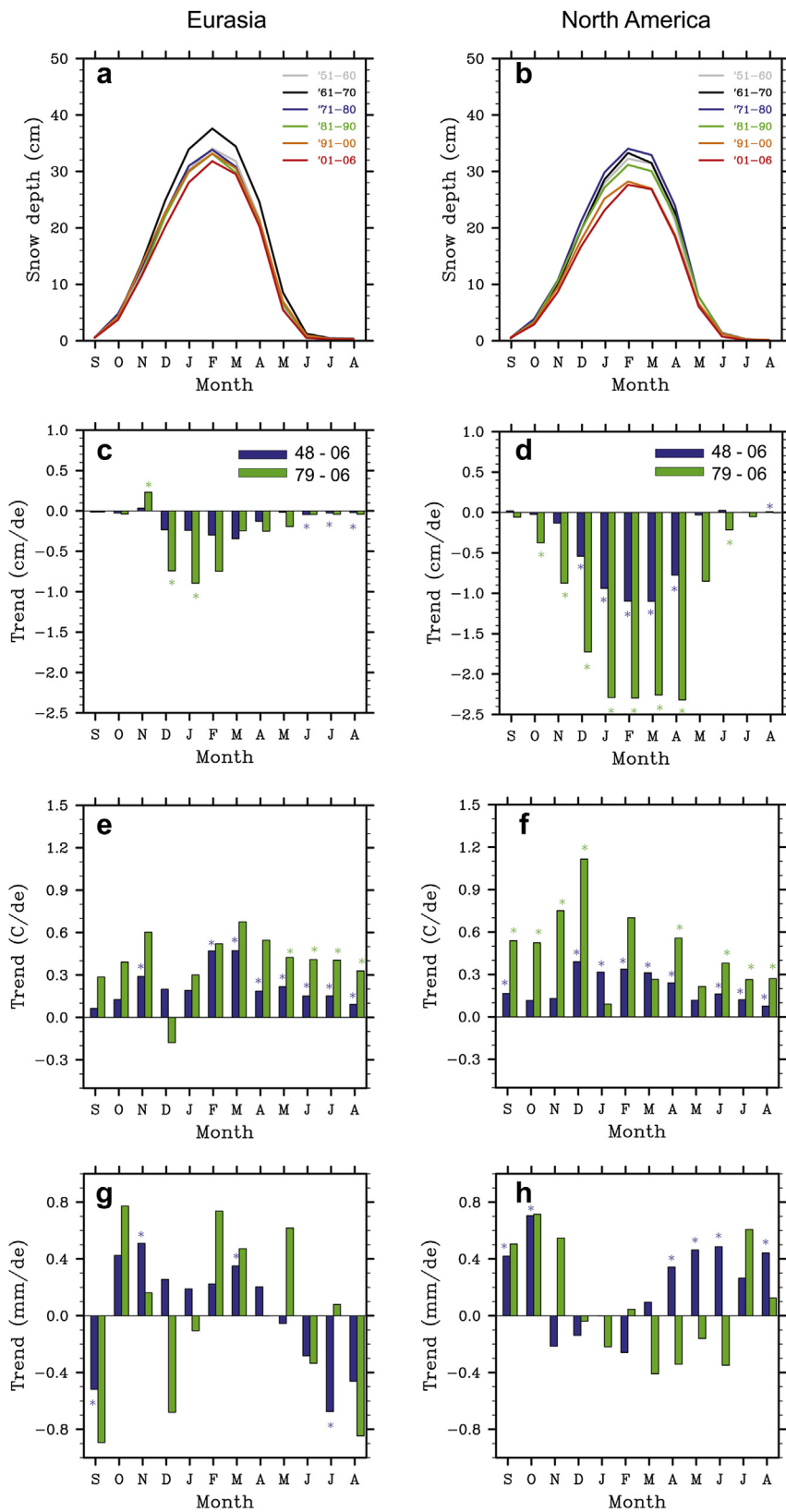
Fig. 4. Monthly variations of decadal averaged snow depth (a, b) and trends of snow depth (c and d), air temperature (e and f), and precipitation (g and h) during two periods (i.e., 1948−2006 and 1979−2006). The left and right panels represent Eurasia and North America, respectively. Asterisks within figures indicate statistical significance at the 95% confidence level.

November, which had a positive trend (Fig. 4c). SAT also increased (Fig. 4e), as it did in NA. However, the magnitude of the decrease in SND was considerably lower than in NA (Fig. 4d), probably as a result of the increased P_G in the autumn and winter (Fig. 4g). While the SND trends in November–January during the 1979–2006 period were statistically significant, no statistical significance was found for the trends of SAT and P_G in the autumn and winter months of the same period.

The SND during 1979–2006 shows large heterogeneous spatial trends for autumn (Fig. 5a) and winter (Fig. 5b). In autumn, the region where the trend of SND was significant (either positive or negative) was concentrated in the northernmost regions >60°N. In EUR the regions with a positive trend were widespread, while the trend in NA was generally negative. The increase in SND over Siberia (Fig. 5a) was consistent with the spatial patterns suggested by Bulygina et al. (2009), who documented an increase in the duration of snow cover over central Siberia and the Far East. In the winter, the areas with a negative trend in SND increased in both EUR and NA (Fig. 5b). Particularly in southwestern Canada, where the trend of SND in the autumn was positive, there was a change to a strong negative trend that was statistically significant. In northern EUR, the area with a positive trend in winter SND also reduced relative to the autumn, and the negative trend of SND in northern Europe was further strengthened. By contrast, areas with a positive trend in SND increased over southern Siberia.

4.3. The influence of diminishing Arctic sea ice on snow depth

After summers with a below-normal SIE, the fluxes of heat and moisture from the sea surface to the atmosphere are anomalously large (Francis et al., 2009). The additional heat transfer into the atmosphere leads to strong stability in the lower atmosphere, which limits vertical mixing (Francis et al., 2009; Screen and Simmonds, 2010). The Arctic warming was greatest in autumn and winter, and signals of this warming were not confined to the sea but also extended to the Arctic boreal regions (Screen and Simmonds, 2010). The composite differences in autumn mean air temperatures after summers when the SIE was less than, and greater than, one standard deviation from the mean of the 1979–2006 period (Fig. 1) are shown in Fig. 6a and d. Using the actual SIE, the composites reveal large areas with positive temperature differences over the Arctic land surface (Fig. 6a). The largest differences exceeding 3 °C were found over far eastern Siberia, western Alaska, and the Canadian Archipelago. These areas belong to the Pacific and Atlantic marginal ice zones, where ice loss has been most pronounced (Liu et al., 2012). The composite analysis, using detrended ice extents, replaced most regions of positive temperature differences with negative values, with the exception of Alaska (Fig. 6d). This was particularly significant for the ambient regions of Hudson Bay and north-central Siberia, where the maximum difference was 5 °C or
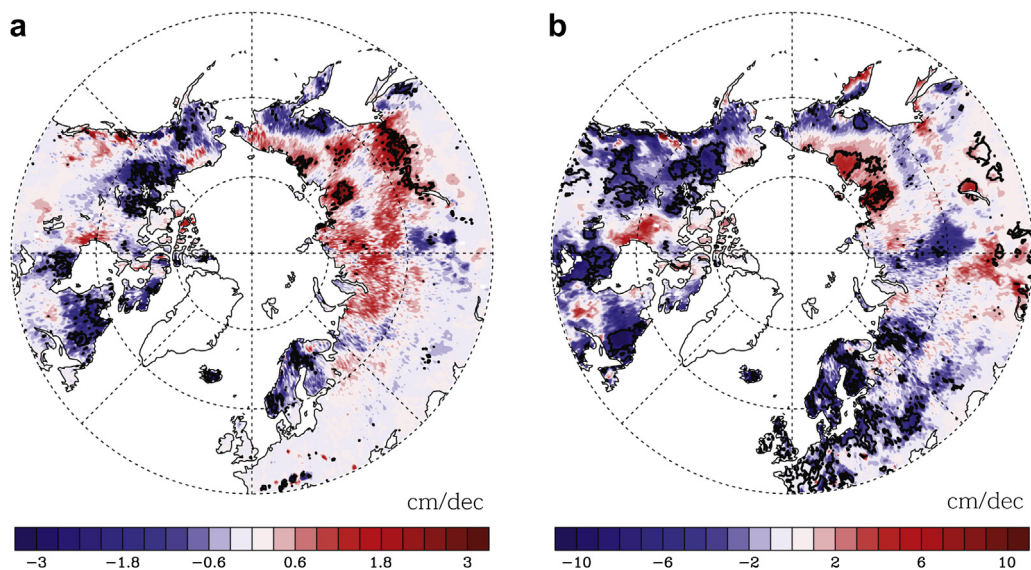

Fig. 5. Linear trends of averaged snow depth in autumn (September–November) (a) and winter (December–February) (b) during the period of 1979–2006. Regions within contours denote points above the 95% confidence level.
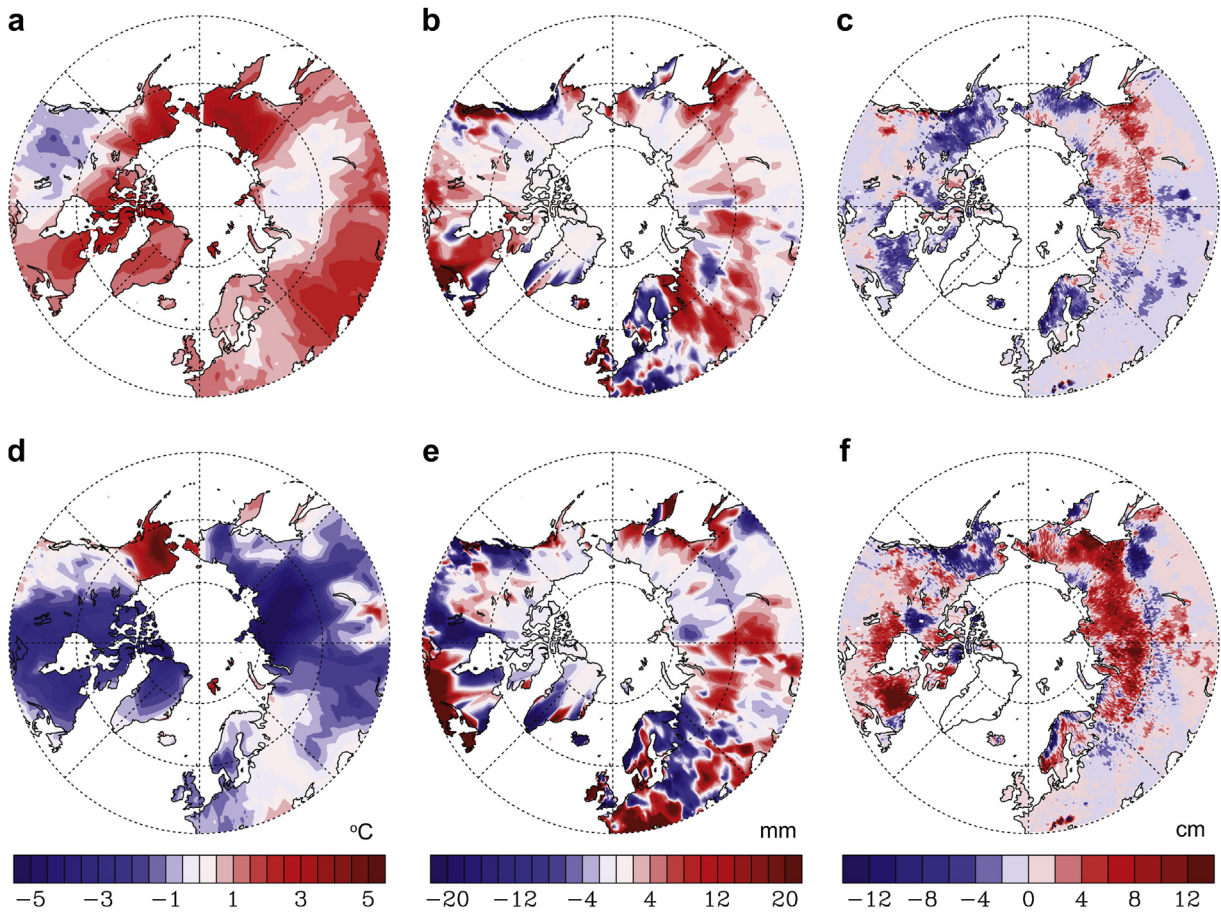
Fig. 6. The difference between composites for autumn (September–November) following Septembers with actual (top) and detrended (bottom) ice extents that were less than and greater than one standard deviation from the 1979–2006 period mean surface air temperature (a and d), precipitation (b and d), and mean snow depth (c and f), composited for low-ice summers minus high-ice summers.

more. This result suggests that the response in these regions is a symptom of the large-scale warming tendency related to the SIE trend (Francis et al., 2009).

Increases in atmospheric water vapor are related to the sea ice loss and enhance the warming in the lower part of the atmosphere during summer and early autumn (Screen and Simmonds, 2010). An increase in the atmospheric water vapor content enhances the emission of longwave radiation to the surface (Francis et al., 2009), resulting in surface warming. The warming would in turn be expected to affect large-scale atmospheric circulation and ultimately influence the weather of the Arctic region. This is evident from the composite differences in the autumnal P_G during reduced-versus-extensive ice years, with and without the trends in ice extent (Fig. 6b and e). The composite differences using the actual SIE trend identified the increase in autumnal P_G over much of the terrestrial Arctic (Fig. 6b), when compared to the composites using the detrended ice extents (Fig. 6e). The

increase in the autumnal P_G was significant in the ambient regions of Hudson Bay, central Siberia, and western EUR (Fig. 6b). The increase appears to be associated with the trend of ice extent. Recent studies have linked decreasing sea ice to increases in autumn cloud cover over the Arctic (Levinson and Lawrimore, 2008) and in precipitating clouds over Siberia (Eastman and Warren, 2010; Stroeve et al., 2011). Modeling studies (Ghatak et al., 2010; Orsolini et al., 2011) have also illustrated that the reduction in sea ice can increase autumnal snowfall over Siberia (Fig. 5a). Interestingly, the increase in P_G in eastern Canada and western EUR is reminiscent of the North Atlantic Oscillation (NAO) (Hurrell, 1995). When the NAO index is in a positive phase, the pressure difference in the northeastern Atlantic is large, consequently increasing storm frequency (Francis et al., 2009).

The composite differences in autumnal SND over northern Siberia were positively anomalous when
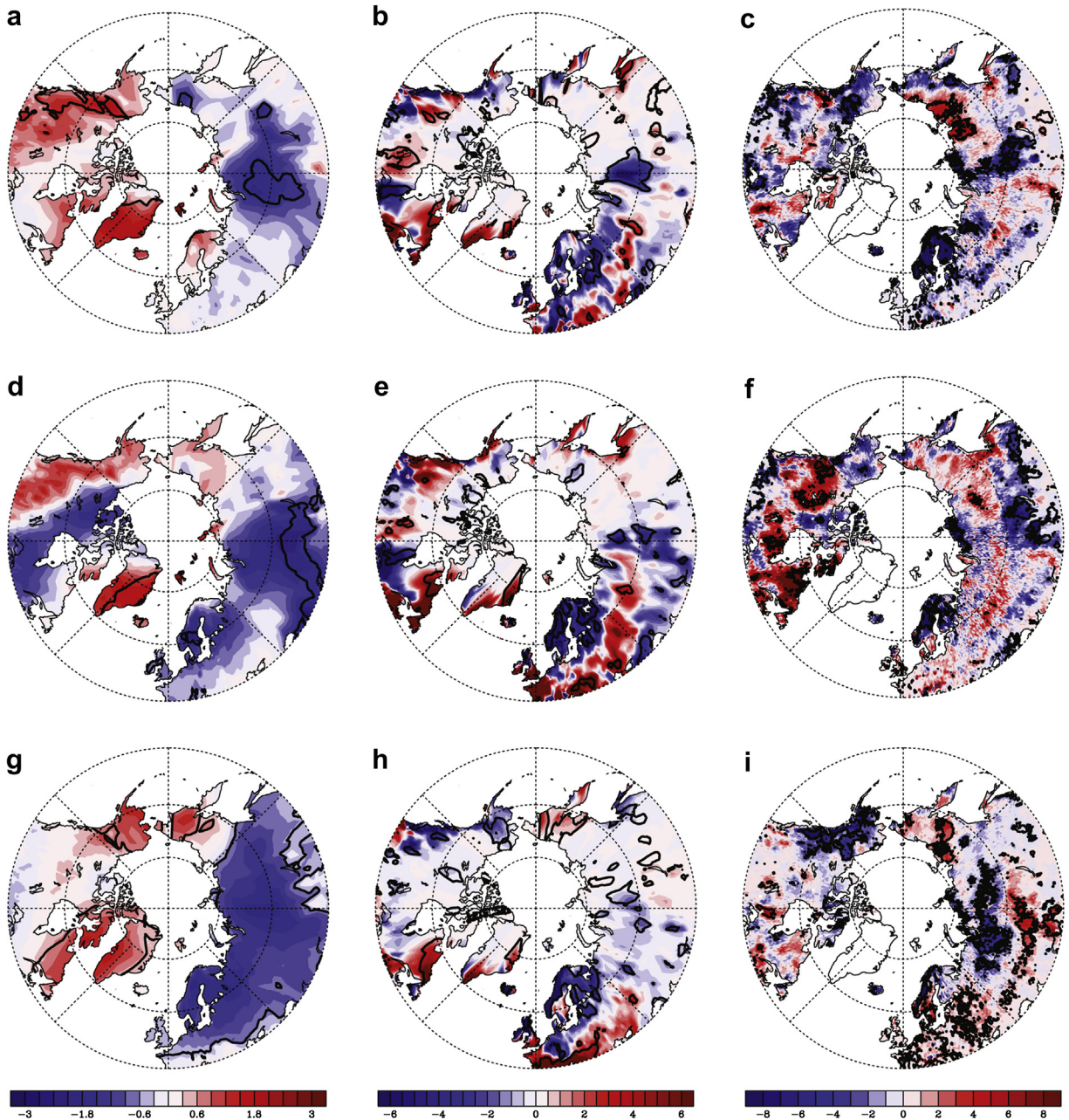
Fig. 7. Linear regressions of averaged surface air temperature (°C/mil. km^2) in winter (December–February) (a, d, and g), precipitation (mm/mil. km^2) (b, e, and h), and mean snow depth (cm/mil. km^2) (c, f, and i) on the September sea ice extent (top), the detrended sea ice extent (middle), and winter AO index (bottom). Regions within contours denote points above the 95% confidence level.

using actual (Fig. 6c) or detrended (Fig. 6f) ice extents. The magnitudes of the composite differences in SND were larger over much of the Arctic land surface when the trend of SIE was not included (Fig. 6f). In contrast, when the actual trend was considered, the area of the positive anomaly in SND over Siberia decreased. This means that the warming associated with the reduced ice extent contributed to the decrease in SND, which was significant for northern Canada and western and far eastern Siberia, where the response of temperature to sea ice loss was substantial (Fig. 6a). For example, in northeastern Canada, the difference in SND using the detrended ice extent was +10 cm or more (Fig. 6f), whereas using the actual ice extent it was −4−0 cm
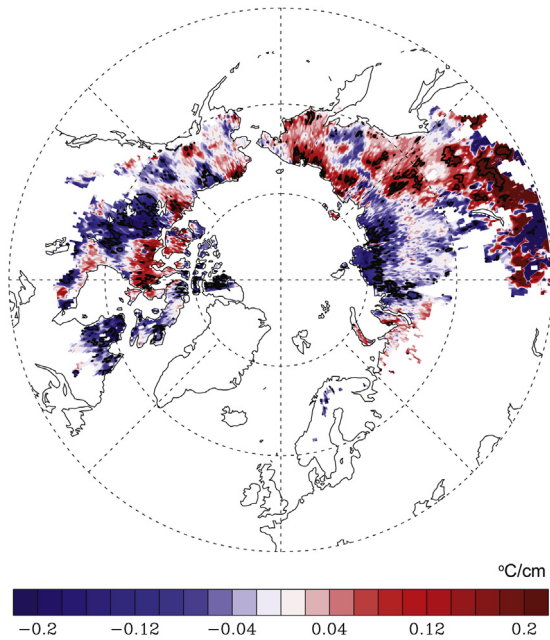
Fig. 8. Linear regression between detrended mean snow depth in autumn (September−November) and soil temperature at 1.2 m depth in the following summer (June−August) during the period of 1979−2006. Regions within contours denote points above the 95% confidence level.

(Fig. 6c). Higher temperatures would primarily increase the fraction of rainfall, rather than snowfall, when precipitation occurs, and would ultimately retard the accumulation of snow. Simulations by Park et al. (2012a) indicated that the timing of the onset of snow over the Arctic land surface was delayed by a maximum of eight days since 1989, due to the warming temperatures. Furthermore, warming increases sublimation from the snow surface, consequently decreasing SND. SND in Alaska exhibited the strongest negative differences when using both actual (Fig. 6c) and detrended (Fig. 6f) ice extents, which seems to be associated with the higher temperatures (Fig. 6a and d).

The memory mechanism that extends the influence of the reduced ice extent into winter has previously been explained by several studies (Deser et al., 2007; Francis et al., 2009; Peng and Whitaker, 1999). The heating of the lower atmosphere associated with the sea ice loss increases the vertical thickness of the lower troposphere, which results in higher geopotential heights of the ice-free upper pressure surfaces and reduces the poleward temperature gradient between the mid- and high latitudes. A reduction of SIE-induced influences on winter weather were found in the linear regressions of inverted SIE with SAT, P_G, and SND

during the following winter, where the trended (Fig. 7, top) and detrended (Fig. 7, middle) SIEs in September were used. The regression values represent changes in variables corresponding to a one million-km^2 change in SIE. The regression indicated that the actual SIE resulted in warming in NA and cooling in EUR (Fig. 7a). Conversely, when the trend of SIE is removed, an increase in the winter SAT occurred over far eastern Siberia, while cold air developed over eastern NA and the Scandinavian Peninsula (Fig. 7d). Temperature anomalies in central Siberia were 2−3 °C below normal, in association with the SIE decrease (Fig. 7a and d). The increase in SAT in northeastern Canada and Greenland was influenced by incursions of warm air masses from the North Atlantic in association with low ice coverage (Liu et al., 2012). The regression of winter SAT anomalies onto the winter AO (Fig. 7g) produced a completely different map from that of the actual SIE (Fig. 7a). The dipole anomalies of warm SAT over NA and cold SAT over EUR (Fig. 7g) resemble the classical negative trend of the AO pattern (Thompson and Wallace, 2001), which is forced partly by the increase in Eurasian snow cover during autumn (Cohen et al., 2007).

The regression between AO and P_G indicates higher positive values over northeastern Canada, southern Europe, and far eastern Siberia. The remaining regions exhibited negative or weak positive regressions (Fig. 7h). The influence of SIE on P_G was similar in the two regressions (Fig. 7b and e). However, it tends to result in a higher P_G over the Canadian region when the trend of SIE is removed (Fig. 7e). The reduction in sea ice produced a zone of wet winters from the seashore of the Sea of Okhotsk across the southern seashore of Alaska, over southern Canada to western EUR (Fig. 7b and e). This pattern of P_G was similar to the North Pacific pattern. Meanwhile, areas of negative anomalies were evident over southern Hudson Bay, northern Europe, and southeastern EUR (Fig. 7b and e).

A regression of SIE with winter SND (Fig. 7c) was similar to the P_G regression (Fig. 7b). However, the SND variability is complicated as increases in P_G also contribute to greater SND. This is because the increased temperature associated with sea ice loss can readily offset the impact of P_G on SND. The actual effects of the higher temperatures were observed in the decreased SND in Alaska and southern Canada (Fig. 7c). The decreased SIE resulted in a significant increase in SND in northeastern Siberia (Fig. 7c), where SND anomalies were up to 8 cm above normal in association with a one million km^2 decrease in the

SIE. The detrended SIE resulted in a significant increase in SND over the Canadian region, excluding the Arctic islands (Fig. 7f). An increase in SND anomalies was also found over western EUR (Fig. 7f). The regression indicated an increase in SND over eastern Siberia (Fig. 7f), as shown in Fig. 7c, which suggests that SND in the region is closely correlated with the reduction of SIE.

Recent studies have suggested that the negative trend in the AO is correlated to decreasing Arctic sea ice (Overland and Wang, 2010; Petoukhov and Semenov, 2010). Associated with the AO, there is increased SND during winter over much of the southern Arctic land surface, particularly southwestern Canada and south-central Siberia (Fig. 7i), which contrasts noticeably with the regression of SIE onto winter SND shown in Fig. 7c. This difference was expected because the decrease in autumn SIE clearly indicates differences in the interannual variability relative to the winter AO (Fig. 1), and the winter AO and the detrended SIE are weakly correlated (0.17). Interestingly, the regression of AO with SND (Fig. 7i) is reminiscent of that expected for negative AO patterns; for example, when the winter AO has a negative trend, the frequency of storms in the middle latitudes is increased (Thompson and Wallace, 2001).

5. Discussion

As illustrated in Fig. 7c, the contribution of the reduction in SIE to the increase in SND was evident for the northernmost terrestrial regions, matching the regions where P_G regressed with SIE was positively anomalous (Fig. 7b). The rapid retreat of sea ice in summer and the slow ice growth during autumn enhanced the latent heat flux from the ocean surface to the atmosphere (Screen and Simmonds, 2010), increasing lower tropospheric moisture over the Arctic, which combines with the effect of the Clausius–Clapeyron relationship to enhance the likelihood of anomalous snowstorm events. The increase in available moisture could potentially lead to higher precipitation efficiency over the Arctic. The reduction in SIE contributed to the increase in autumnal P_G over much of the terrestrial Arctic (Fig. 6b), which was linked to higher SND (Fig. 6c). Finnis et al. (2007) indicated that high-latitude regions experience increased P_G from storms during autumn owing to the availability of atmospheric moisture associated with the diminishing sea ice. The diminished sea ice in turn recovers during late autumn and early winter. During the ice recovery, the humidity of the Arctic air masses increases, which

may be connected to the variability of winter P_G over the Arctic. A recent study noted that the declining Arctic sea ice is directly connected to a shift to a more meridional atmospheric circulation pattern in winter, rather than zonal symmetry (Liu et al., 2012). The modified circulation pattern transports the moisture induced in autumn southward from the Arctic. Kurita (2011), using water isotopes as tracers, found that water vapor in eastern Siberia during ice growth originated from the Arctic Ocean. Observational data have also shown that following an anomalously low ice extent in autumn, a pronounced increase in humidity occurred in far eastern Siberia, northern/eastern Europe, and western Alaska (Liu et al., 2012). The increased humidity would provide moisture sources to the regions, resulting in higher SND. This suggests that a first-order link between sea ice variability and winter P_G potentially contributes to SND variability, through the changed circulation pattern.

The detrended SIE resulted in strong increases in winter SND over large parts of Canada (Fig. 7f), which was clearly distinguished from the negative trend of SND (Fig. 5b). In particular, the increase in SND in western Canada was associated with P_G patterns modified by the reduction in Arctic sea ice. Western Canada is known to be influenced by a moisture influx associated with the Aleutian low. Francis et al. (2009) noted that the Aleutian low during autumn was weaker following summers with less ice. However, intraseasonal modeling studies have suggested that as Arctic sea ice cover is reduced, precipitation patterns over western NA shift toward drier conditions in southwestern NA and wetter conditions in northwestern NA (Sewall, 2005). In reality, increases in P_G in western Canada were identified during autumn (Fig. 6b) and winter (Fig. 7e) and are responsible for the increase in winter SND over Canada (Fig. 7f), which differs from the general negative trend of SND (Fig. 5b).

The diminishing Arctic sea ice has simultaneously contributed to the increase in SAT (Serreze and Francis, 2006; Serreze et al., 2009) alongside the increase in P_G (Fig. 7b). The increase in winter SAT over northwestern NA was remarkably significant (Figs. 2b and 4f) relative to the cold Siberia region (Fig. 6a). The variability of SND is sensitive to the radiative balance (Groisman et al., 1994), surface energy fluxes (Dyer and Mote, 2002), and variations in air temperature (Brown and Goodison, 1996). The increased SAT can overwhelm the effect of the increased P_G (Fig. 4), thereby decreasing SND. Under warming conditions, snowfall is partially or wholly replaced by rain, and snowmelt is increased, resulting

in a diminished snowpack. A significant decrease in SND over northwestern Canada in response to rising air temperatures has been observed (Dyer and Mote, 2006). Park et al. (2012a) have also suggested the influence of warming temperatures on the negative trend in winter SND over much of NA. The Community Climate System Model (CCSM3) future simulations showed reductions of snow cover at the hemispheric scale outside the Siberian region, which correlated with the reduction of Arctic sea ice (Ghatak et al., 2010).

The SND in eastern Siberia increased during autumn (Fig. 5a) in response to the reduction in sea ice, and these SND conditions continued throughout the winter season (Fig. 7c). Larger snow depth over Siberia was also identified by future simulation experiments. Global climate models have projected an increase in snow water equivalent over northern Siberia, responding to sea ice loss in the 21st century (Callaghan et al., 2011; Deser et al., 2010; Räisänen, 2008). Although temperature has increased, the Siberian regions are sufficiently cold to maintain snow cover during the winter season (Fig. 7a). The cold winter in Siberia is closely related to the aforementioned circulation changes. Under the diminishing Arctic sea ice conditions, the weakened westerly winds tend to exhibit broad meanders that are likely to form blocking circulations in Eastern Europe, central Siberia, and southern Alaska. Such blocking favors more frequent incursions of cold air masses from the Arctic into the middle and low latitudes of northern continents (Liu et al., 2012). In these cold conditions, a more moisture-laden atmosphere, resulting from sea ice loss in autumn, contributes to the increase in snowfall.

Snow is a strong insulator, limiting heat transfer between the atmosphere and the ground. The variability of SND during the early winter can either amplify or mitigate soil warming, which is likely to persist into the following summer as a memory in the soil system. To explore the insulation effect, the detrended mean SND during September–November was linearly regressed with the mean soil temperature at 1.2 m of the following summer (i.e., June–August) over the 1979–2006 period (Fig. 8). The investigation was limited to the permafrost area as defined by the model. Strong insulation effects of SND on soil temperature were discovered over east Siberia, where SND in autumn exhibited an increasing trend (Fig. 5a). The insulation effect reached a maximum of 0.2 °C or more per 1 cm SND in south Siberia. The corresponding value in northeastern Siberia was 0.10–0.15 °C. In NA, a positive relationship between

autumnal SND and soil temperature was determined in the northernmost regions; for example, soil temperature in the Canadian Arctic increased by 0.06–0.14 °C per 1 cm SND. By contrast, the reduced SND in western Alaska resulted in soil cooling. Soil temperature in southern Canada, with a lower, SND increased, while in central Siberia, it was negatively regressed with the higher autumnal SND (Fig. 5a). It seems that the negative anomalies of soil temperature in central Siberia were associated with the cold air temperature (Fig. 2a) and the reduced SND (Fig. 5b) during the subsequent winter season. Likewise, an increase or decrease in SND was not necessarily connected to soil warming or cooling (as shown in Fig. 8) because soil temperature has a complex relationship with air temperature, precipitation, and soil moisture during the subsequent winter and next summer season. Park et al. (2012b) also found that the influence of soil moisture on the thermal state of summer soil can override the effect of air temperature. However, there was an evident empirical relationship, where the increased SND was tied to soil warming, at least in eastern Siberia and the Canadian Arctic, suggesting that the role of decreasing sea ice is behind the relationship between SND and soil temperature. Lawrence and Slater (2010) suggested that for the latter half of the twentieth century, snow state variations explain as much as 50–100% of total soil temperature variations. In a future SIE experiment for Alaska, snowpack in the winter season increased significantly, which contributed to warmer soil temperatures for most seasons by insulating the land surface (Higgins and Cassano, 2012).

6. Conclusion

In this study, we evaluated how the diminishing SIE in September has influenced SND over Arctic terrestrial regions during the period of 1979–2006. During this period, the Arctic sea ice in September continuously decreased, and the simulated SNDs in EUR and NA also produced decreasing trends. The decrease in SND was more significant in NA than in EUR and was closely correlated to temperature warming. Regional increases in SND were found in eastern Siberia, northern Alaska, and the Canadian Arctic amid the reduction in Arctic sea ice. Diminishing Arctic sea ice contributed to the increase in P_G, which was linked to snowy winters over large parts of the northern terrestrial Arctic. Furthermore, linear regression of detrended SIE with SND indicated that the reduction in sea ice resulted in a positively anomalous SND in eastern

Siberia, as well as Canadian regions where a negative trend of SND was clear. This study demonstrates that diminishing sea ice definitely affected SND in the northernmost terrestrial regions.

Regional responses of SAT to reductions in Arctic sea ice were quite different. Temperature in northwestern NA increased anomalously with diminishing sea ice. The warming temperatures over NA overwhelmed the effect of increased P_G, thereby decreasing SND. By contrast, the reduction in sea ice led to cold conditions over Siberian regions in winter. Together with enhanced snowfall, this contributed to an increase in SND in eastern Siberia. The thicker SND in eastern Siberia early in the snow season was linked to soil warming in the following summer. The insulation effect of SND on soil temperature was also found in part of the Canadian Arctic.

Episodes of diminishing sea ice, which have increased SND over eastern Siberia, have been suggested by recent observations and climate modeling results. This study also identified such an episode in the Canadian Arctic. We can conclude definitively that diminishing Arctic sea ice has increased SND in the northernmost terrestrial Arctic during recent decades. The decrease in snow depth on a continental scale, outside of the northernmost regions, suggests a sea ice-related Arctic amplification on the terrestrial Arctic snowpack. If the decline of Arctic sea ice continues as anticipated by global climate models, we can speculate that the variability of terrestrial Arctic snow will intensify, along with warming temperatures and more persistent snowstorms during winter. A better understanding of interactions between the diminishing Arctic sea ice and winter mean statistics (i.e., snow and temperature) is an important area for further research.

Acknowledgment

References

Bekryaev, R., Polyakov, I., Alexeev, V., 2010. Role of polar amplification in long-term surface air temperature variations and modern Arctic warming. J. Clim. 23, 3888—3906. http://dx.doi.org/10.1175/2010JCLI3297.1.

Brown, R., 2000. Northern Hemisphere snow cover variability and change, 1915-97. J. Clim. 13, 2339—2355. http://dx.doi.org/10.1175/1520-0442(2000)013<2339:NHSCVA>2.0.CO;2.

Brown, R., Goodison, B., 1996. Interannual variability in reconstructed Canadian snow cover. 1915—1992. J. Clim. 9, 1299—1318.

Brown, R., Derksen, C., Wang, L., 2010. A multi-data set analysis of variability and change in Arctic spring snow cover extent, 1967-2008. J. Geophys. Res. 115, D16111. http://dx.doi.org/10.1029/2010JD013975.

Bulygina, O., Razuvaev, V., Korshunova, N., 2009. Change in snow cover over northern Eurasia in the last decades. Environ. Res. Lett. 4, 045026. http://dx.doi.org/10.1088/17489326/14/4/045026.

Callaghan, T., Johansson, M., Brown, R., Groisman, P., Labba, N., Radionov, V., 2011. Changing Snow Cover and Its Impacts, in AMAP, 2011, Snow, Water, Ice and Permafrost in the Arctic (SWIPA), 2011 Permafrost in the Arctic (SWIPA): Climate Change and the Cryosphere, Arctic Monitoring and Assessment Programme (AMAP), Oslo, Norway, 538 pp.

Cohen, J., Barlow, M., Kushner, P., Saito, K., 2007. Stratosphere-troposphere coupling and links with Eurasian land-surface variability. J. Clim. 20, 5335—5343.

Cohen, J., Furtado, J., Barlow, M., Alexeev, V., Cherry, J., 2012. Arctic warming, increasing snow cover and widespread boreal winter cooling. Environ. Res. Lett. 7, 014007. http://dx.doi.org/10.1088/1748-9326/1/1/014007.

Comiso, J., Parkinson, C., Gersten, R., Stock, L., 2008. Accelerated decline in the Arctic sea ice cover. Geophys. Res. Lett. 35, L01703. http://dx.doi.org/10.1029/2007GL031972.

Deser, C., Thomas, R., Peng, S., 2007. The transient atmospheric circulation response to North Atlantic SST and sea ice anomalies. J. Clim. 20, 4751—4767.

Deser, C., Tomas, R., Alexander, M., Lawrence, D., 2010. The seasonal atmospheric response to projected Arctic sea ice loss in the late twenty-first century. J. Clim. 23, 333—351. http://dx.doi.org/10.1175/2009JCLI3053.1.

Dyer, J., Mote, T., 2002. Role of energy budget components on snow ablation from a mid-latitude prairie snowpack. Polar Geogr. 26, 87—115.

Dyer, J., Mote, T., 2006. Spatial variability and trends in observed snow depth over North America. Geophys. Res. Lett. 33, L16503. http://dx.doi.org/10.1029/2006GL027258.

Eastman, R., Warren, S., 2010. Interannual variations of Arctic cloud types in relation to sea ice. J. Clim. 23, 4216—4232.

Fetterer, F., Knowles, K., Meier, W., Savoie, M., 2002. Sea Ice Index. National Snow and Ice Data Center, Boulder, CO (updated 2009).

Finnis, J., Holland, M., Serreze, M., Cassano, J., 2007. Response of Northern Hemisphere extratropical cyclone activity and associated precipitation to climate change, as represented by the Community Climate System Model. J. Geophys. Res. 112, G04S42. http://dx.doi.org/10.1029/2006JG000286.

Francis, J., Chan, W., Leathers, D., Miller, J., Veron, D., 2009. Winter Northern Hemisphere weather patterns remember summer Arctic sea-ice extent. Geophys. Res. Lett. 36, L07503. http://dx.doi.org/10.1029/2009GL037274.

Ghatak, D., Frei, A., Gong, G., Stroeve, J., Robinson, D., 2010. On the emergence of an Arctic amplification signal in terrestrial Arctic snow extent. J. Geophys. Res. 11, D24105. http://dx.doi.org/10.1029/2010JD014007.

Groisman, P., Karl, T., Knight, R., 1994. Changes of snow cover, temperature, and radiative heat balance over the Northern Hemisphere. J. Clim. 7, 1633—1656.

Higgins, M., Cassano, J., 2012. Northern Alaskan land surface response to reduced Arctic sea ice extent. Clim. Dyn. 38, 2099—2113. http://dx.doi.org/10.1007/s00382-011-1095-0.

Hirabayashi, Y., Kanae, S., Motoya, K., Masuda, K., Doll, P., 2008. A 59-year (1948-2006) global near-surface meteorological data set

for land surface models. Part I: development of daily forcing and assessment of precipitation intensity. Hydrol. Res. Lett. 2, 36−40.

Hurrell, J., 1995. Decadal trends in the North Atlantic Oscillation: regional temperatures and precipitation. Science 269, 676−679.

Intergovernmental Panel on Climate Change (IPCC), 2008. Climate Change 2007: Synthesis Report. Contribution of Working Groups I, II and III to the Fourth Assessment Report of the Intergovernmental Panel on Climate Change, edited by Core Writing Team, et al., 104 pp., Geneva, Switzerland.

Kitaev, L., Forland, E., Razuvaev, V., Tveito, O., Krueger, O., 2005. Distribution of snow cover over Northern Eurasia. Nord. Hydrol. 36, 311−319.

Kurita, N., 2011. Origin of Arctic water vapor during the ice-growth season. Geophys. Res. Lett. 38, L02709. http://dx.doi.org/10.1029/2010GL046064.

Lawrence, D., Slater, A., 2010. The contribution of snow condition trends to future ground climate. Clim. Dyn. 34. http://dx.doi.org/10.1007/s00382-009-0537-4

Levinson, D., Lawrimore, J., 2008. State of the climate in 2007. Bull. Am. Meteorol. Soc. 89, S1−S179. http://dx.doi.org/10.1175/BAMS-89-7-StateoftheClimate.

Liu, J., Curry, J., Wang, H., Song, M., Horton, R., 2012. Impact of declining Arctic sea ice on winter snowfall. Proc. Natl. Acad. Sci. U.S.A.. http://dx.doi.org/10.1073/pnas.1114910109

McCabe, G., Wolock, G., 2010. Long-term variability in Northern Hemisphere snow cover and associations with warmer winters. Clim. Change 99, 141−153. http://dx.doi.org/10.1007/s10584-009-9675-2.

Orsolini, Y., Senan, R., Benestad, R., Melsom, A., 2011. Autumn atmospheric response to the 2007 low Arctic sea ice extent in coupled ocean-atmosphere hindcasts. Clim. Dyn. 114, D19108. http://dx.doi.org/10.1007/s00382-011-1169-z.

Overland, J., Wang, M., 2010. Large-scale atmospheric circulation changes are associated with the recent loss of Arctic sea ice. Tellus A 62, 1−9.

Park, H., Iijima, Y., Yabuki, H., Ohta, T., Walsh, J., Kodama, Y., Ohata, T., 2011. The application of a coupled hydrological and biogeochemical model (CHANGE) for modeling of energy, water, and CO_2 exchanges over a larch forest in eastern Siberia. J. Geophys. Res. 116, D15102. http://dx.doi.org/10.1029/2010JD015386.

Park, H., Yabuki, H., Ohata, T., 2012a. Analysis of satellite and model datasets for variability and trends in Arctic snow extent and depth, 1948−2006. Polar Sci. 6 (1), 23−37.

Park, H., Walsh, J., Fedorov, A., Sherstiukov, A., Iijima, Y., Ohata, T., 2012b. The influence of climate and hydrological variables on opposite anomaly in active layer thickness between Eurasian and North American watersheds. Cryosphere Discuss. 6, 1−38. http://dx.doi.org/10.5194/tcd-6-1-2012.

Peng, S., Whitaker, J., 1999. Mechanisms determining the atmospheric response to midlatitude SST anomalies. J. Clim. 12, 1393−1408.

Peterson, B., et al., 2002. Increasing river discharge to the Arctic Ocean. Science 298, 2171−2173. http://dx.doi.org/10.1126/science.1077445.

Petoukhov, V., Semenov, V., 2010. A link between reduced Barents-Kara sea ice and cold winter extremes over northern continents. J. Geophys. Res. 115, D21111. http://dx.doi.org/10.1029/2009JD013568.

Räisänen, J., 2008. Warmer climate: less or more snow? Clim. Dyn. 30, 307−319. http://dx.doi.org/10.1007/s00382-007-0289-y.

Schindler, D., Donahue, W., 2006. An impending water crisis in Canada's western prairie provinces. Proc. Natl. Acad. Sci. U.S.A. 103. http://dx.doi.org/10.1073/pnas.0601568103

Screen, J., Simmonds, I., 2010. The central role of diminishing sea ice in recent Arctic temperature amplification. Nature 464 (29). http://dx.doi.org/10.1038/nature09051.

Serreze, M., Francis, J., 2006. The Arctic amplification debate. Clim. Change 76 (3−4), 241−264. http://dx.doi.org/10.1007/s10584-005-9017-y.

Serreze, M., Walsh, J., Chapin, E., Osterkamp, T., Dyugerov, P., Romanovsky, M., Oechel, W., Morison, C., Zhang, T., Barry, R., 2000. Observational evidence of recent change in the northern high-latitude environment. Clim. Change 46, 159−207. http://dx.doi.org/10.1023/A:1005504031923.

Serreze, M., Barrett, A., Stroeve, J., Kindig, D., Holland, M., 2009. The emergence of surface-based Arctic amplification. Cryosphere 3, 11−19. http://dx.doi.org/10.5194/tc-3-11-2009.

Sewall, J., 2005. Precipitation shifts over western North America as a result of declining Arctic sea ice cover: the coupled system response. Earth Interact. 9, 1−23.

Shi, X., Groisman, P., Dery, S., Lettenmaier, D., 2011. The role of surface energy fluxes in pan-Arctic snow cover changes. Environ. Res. Lett. 6, 035204. http://dx.doi.org/10.1088/1748-9326/6/3/035204.

Storck, P., Lettenmaier, D., Bolton, S., 2002. Measurement of snow interception and canopy effects on snow accumulation and melt in a mountainous maritime climate, Oregon, United States. Water Resour. Res. 38. http://dx.doi.org/10.1029/2002WR001281

Stroeve, J., Serreze, M., Barrett, A., Kindig, D., 2011. Attribution of recent changes in autumn cyclone associated precipitation in the Arctic. Tellus A 63, 1−11.

Sturm, M., Racine, C., Tape, K., 2001. Climate change − increasing shrub abundance in the Arctic. Nature 411, 546−547. http://dx.doi.org/10.1038/35079180.

Thompson, D., Wallace, J., 1998. The Arctic Oscillation signature in the wintertime geopotential height and temperature fields. Geophys. Res. Lett. 25, 1297−1300.

Thompson, D., Wallace, J., 2001. Regional climate impacts of the Northern Hemisphere Annular Mode. Science 293, 85−89.

Ye, H., 2001. Increases in snow season length due to earlier first snow and later last snow dates over North Central and Northwest Asia during 1937-94. Geophys. Res. Lett. 28 (3), 551−554. http://dx.doi.org/10.1029/2000GL012036.